doi:10.1093/jmcb/mjp002
Published online June 10, 2009

Article

PAMAM Nanoparticles Promote Acute Lung Injury by Inducing Autophagic Cell Death through the Akt-TSC2-mTOR Signaling Pathway

Chenggang Li[1,†], Haolin Liu[1,†], Yang Sun[1,†], Hongliang Wang[1], Feng Guo[1], Shuan Rao[1], Jiejie Deng[1], Yanli Zhang[1], Yufa Miao[2], Chenying Guo[3], Jie Meng[4], Xiping Chen[5], Limin Li[5], Dangsheng Li[6], Haiyan Xu[4,*], Heng Wang[3,*], Bo Li[2], and Chengyu Jiang[1,*]

1 State Key Laboratory of Medical Molecular Biology, Department of Biochemistry and Molecular Biology, Institute of Basic Medical Sciences, Chinese Academy of Medical Sciences, Peking Union Medical College; Beijing 100005, China
2 National Center for Safety Evaluation of Drugs, National Institute for the Control of Pharmaceutical and Biological Products, Hongda Middle Street A8, Beijing Economic and Technological Development Area, Beijing 100176, China
3 Molecular Parasitology Laboratory, Department of Etiology, Institute of Basic Medical Sciences, Chinese Academy of Medical Sciences, Peking Union Medical College, Beijing 100005, China
4 Department of Biological Science and Medical Engineering, Institute of Basic Medical Sciences, Chinese Academy of Medical Sciences, Peking Union Medical College; Beijing 100005, China
5 Department of Pathology, Institute of Basic Medical Sciences, Chinese Academy of Medical Sciences, Peking Union Medical College, Beijing 100005, China
6 Shanghai Institute for Biological Sciences, Chinese Academy of Sciences, Shanghai 200031, China
* Correspondence to: Chengyu Jiang, Tel: 10-65296908; Fax: 10-65276551; E-mail: jiang@pumc.edu.cn; Heng Wang, E-mail: hengwang@pumc.edu.cn; Haiyan Xu, E-mail: xuhy@pumc.edu.cn

Nanotechnology is an important and emerging industry with a projected annual market of around one trillion US dollars by 2011–2015. Concerns about the toxicity of nanomaterials in humans, however, have recently been raised. Although studies of nanoparticle toxicity have focused on lung disease the molecular link between nanoparticle exposure and lung injury remained unclear. In this report, we show that cationic Starburst polyamidoamine dendrimer (PAMAM), a class of nanomaterials that are being widely developed for clinical applications can induce acute lung injury *in vivo*. PAMAM triggers autophagic cell death by deregulating the Akt-TSC2-mTOR signaling pathway. The autophagy inhibitor 3-methyladenine rescued PAMAM dendrimer-induced cell death and ameliorated acute lung injury caused by PAMAM in mice. Our data provide a molecular explanation for nanoparticle-induced lung injury, and suggest potential remedies to address the growing concerns of nanotechnology safety.

Keywords: PAMAM, nanoparticles, autophagy, acute lung injury, Akt, TSC2, mTOR

Introduction

Nanomaterials are used in many different products, including sporting goods, tires, cosmetics and electronics, as well as in medicine for diagnosis, imaging and drug delivery (Freitas, 2005; Gelperina et al., 2005; Svenson and Tomalia, 2005). In the pharmaceutical industry, dendrimers are of particular interest for applications in gene transfer, drug delivery and imaging because of their well-defined particle size and shape (Svenson and Tomalia, 2005; Gao et al., 2008). Among them, Starburst polyamidoamine (PAMAM) dendrimers are especially important because they are uniquely based on an ethylenediamine core and repeated amidoamine branching, which binds well to DNA or proteins. PAMAM dendrimers are often referred to as 'artificial proteins' (Hecht and Frechet, 2001) and PAMAM generation 3 (G3), G4 and G5 are similar in size and shape to insulin, cytochrome C and hemoglobin, respectively. The close match of PAMAM G7–G10 in size and shape with histone clusters accounts for the high stability of DNA–PAMAM complexes. PAMAM G4, G5 and G6 also possess nanoscale container property, which accounts for their function as ideal drug-delivery vectors. Indeed, PAMAM dendrimer nanomaterials are now being developed for the pharmaceutical industry, as drugs or therapeutic components for anti-cancer and anti-pathogen treatments (Cheng et al., 2008; Cheng et al., 2007; Duncan and Izzo, 2005; Xu et al., 2007) (http://www.starpharma.com/vivagel.asp). PAMAM dendrimers are also commercially available (Dendritech) as whole (cationic) or half (anionic) generation polymers (Malik et al., 2000). Here we examine the toxicity of 12 PAMAM dendrimers, and investigate in detail the underlying molecular mechanisms of cell and host toxicity caused by PAMAM G3.

†These authors contributed equally to this work.
Received February 10, 2009. Revised April 14, 2009. Accepted April 16, 2009.

Results

Some PAMAM nanoparticles are toxic

Since the *in vivo* tissue distribution of dendrimer G5 has been reported to show high concentrations in lung tissue and the toxicity of dendrimers has been mostly implicated in lungs (Nigavekar et al., 2004), we first examined the cell survival rate of human lung adenocarcinoma A549 cells treated with a variety of PAMAM dendrimers including both cationic and anionic generations G1, G2, G3, G4, G5, G6, G7, G8, G3.5, G4.5, G5.5 and G7.5 (Figure 1A). Cell death was observed upon treatment with most of the cationic PAMAM dendrimers, including G3, G4, G5, G6, G7 and G8; but not with anionic derivatives. We selected PAMAM G3 representing toxic cationic PAMAM series and G5.5 representing anionic PAMAM series for studying mechanisms of the toxicity. To determine whether cationic PAMAM dendrimers induce apoptosis, we treated A549 cells with cationic PAMAM G3, and assessed DNA fragmentation (Figure 1B) and caspase-3 activity (Figure 1C), which are hallmarks of apoptosis. We used 6% DMSO as the positive control (Trubiani et al., 1999; Aita et al., 2005). Interestingly, we did not observe any apoptosis in cells treated with PAMAM G3, suggesting that PAMAM-induced cell death occurs via an alternative pathway (Figure 1B and C).

Toxic PAMAM nanoparticles induce autophagic cell death in A549 cells

Autophagy is an intracellular mechanism in which cells degrade proteins and organelles by engulfing them in double-membrane vacuoles known as autophagosomes (Bergmann, 2007). In recent years, it has been postulated that excessive autophagy can directly promote cell death independently of the apoptotic pathway (Baehrecke, 2005). Various nanoparticles, such as quantum dots and nano neodymium oxide, have been shown to induce autophagy (Chen et al., 2005; Seleverstov et al., 2006; Zabirnyk et al., 2007), although the underlying mechanisms are unknown. To determine whether PAMAM dendrimers can also induce autophagy, we cultured human lung A549 cells with PAMAM dendrimers and processed samples for analysis by transmission electron microscopy. Cationic PAMAM G3 specifically induced the accumulation of autophagosomes in cells, which is a hallmark of autophagy, while anionic PAMAM G5.5 and the vehicle control failed to do so (Figure 2A and B). Treatment with the autophagy inhibitor 3MA significantly reduced the percentage of autophagosome-positive cells induced by PAMAM G3 (Figure 2A and B). As an independent assessment of autophagy, we analysed the expression of the microtubule-associated protein 1 light chain 3 (LC3), a marker protein for autophagy (Asanuma et al., 2003).

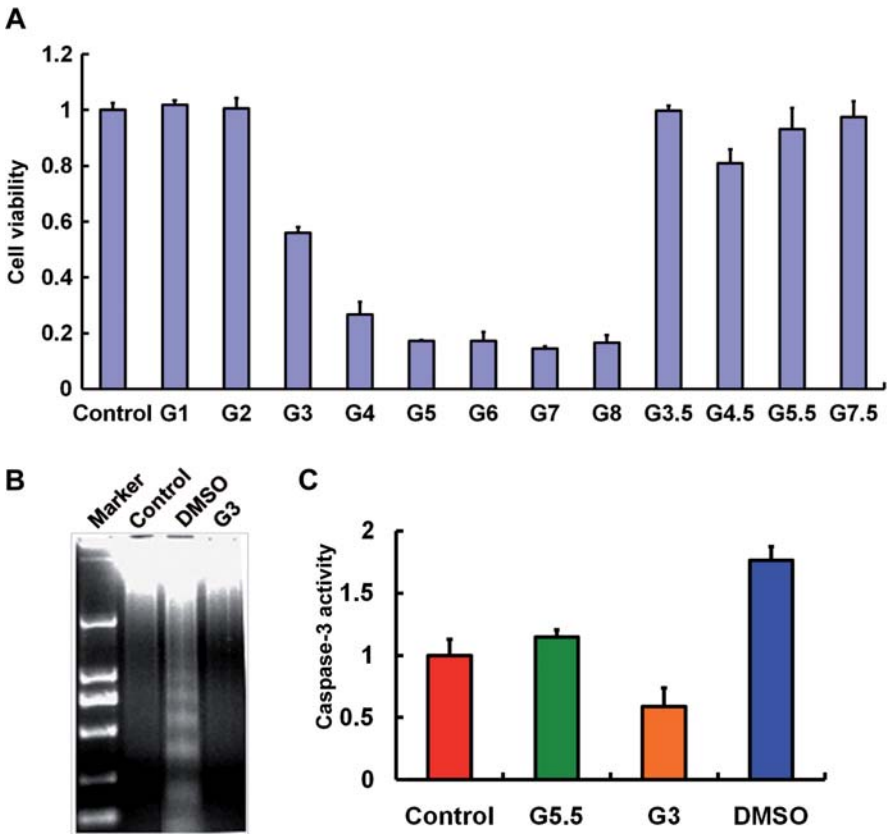

Figure 1 PAMAM nanoparticles induce cell death in human lung adenocarcinoma A549 cells. (**A**) MTT assay of A549 cells treated with different generations of PAMAM nanoparticles (100 μg/ml) for 24 h. (**B**) Genomic DNA electrophoresis of control, DMSO and PAMAM G3 (100 μg/ml)-treated A549 cells. DMSO is used as a positive control. (**C**) Caspase-3 activity after control, PAMAM G5.5 (100 μg/ml), PAMAM G3 (100 μg/ml) and DMSO treatment for 24 h.

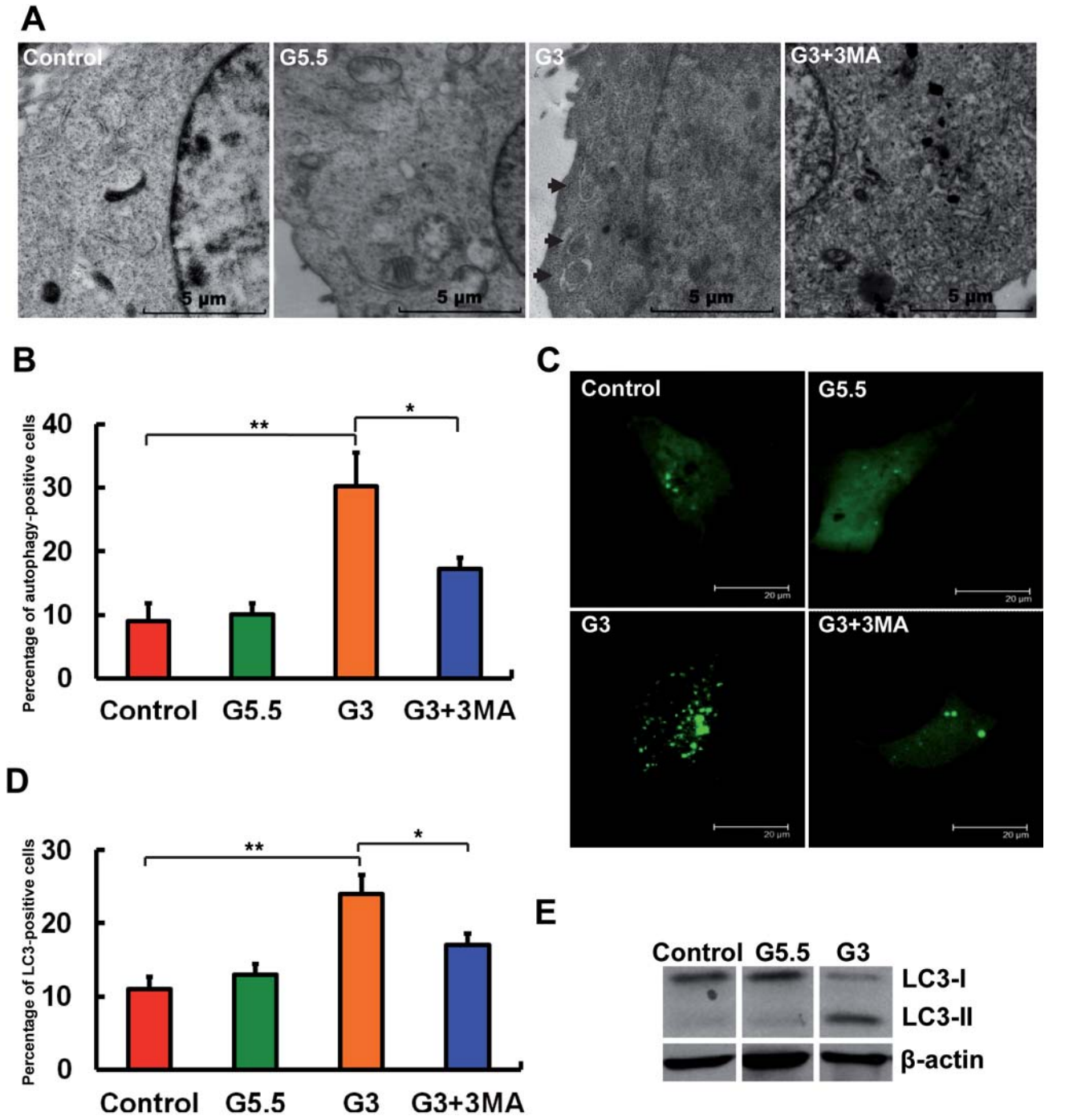

Figure 2 PAMAM nanoparticle G3 induces autophagy in human lung adenocarcinoma A549 cells. (**A**) Electron microscopy images of A549 cells treated with control, PAMAM G5.5 (100 μg/ml), PAMAM G3 (100 μg/ml) and PAMAM G3 (100 μg/ml) plus 3-methyladenine (3MA, 10 mM) for 24 h. Arrows indicate autophagosomes. (**B**) Percentage of cells containing autophagic vesicles after treatment with control, PAMAM G5.5, PAMAM G3 and PAMAM G3 plus 3MA. $^{**}P < 0.01$ and $^{*}P < 0.05$. (**C**) Confocal images of control, PAMAM G5.5 (30 μg/ml), PAMAM G3 (30 μg/ml) and PAMAM G3 (30 μg/ml) plus 3MA (10 mM)-treated A549 cells expressing transfected LC3-EGFP; PAMAM dendrimer treatment was for 24 h. (**D**) Percentage of LC3-positive cells after control, PAMAM G5.5, PAMAM G3 and PAMAM G3 plus 3MA treatment. $^{**}P < 0.01$ and $^{*}P < 0.05$. (**E**) Western blots of lysates of PAMAM dendrimer (100 μg/ml)-treated and control A549 cells probed with anti-LC3-I & II; PAMAM dendrimer treatment was for 4 h.

Confocal microscopy showed that cationic PAMAM G3-induced LC3 aggregation in A549 cells (Figure 2C and D). Treatment with the autophagy inhibitor 3MA decreased these LC3 aggregations (Figure 2C and D). The increase of LC3-II protein is an alternative assay for identifying the autophagy process (Asanuma et al., 2003). Western blots of cell lysates confirmed an increase in LC3-II induced by PAMAM G3 when compared with the vehicle control and PAMAM G5.5 (Figure 2E). Taken together, these results show that cationic PAMAM G3 dendrimers can induce autophagy in human lung adenocarcinoma A549 cells.

Autophagy can serve as a cell-survival mechanism apart from inducing cell death. To test whether PAMAM G3-induced cell death is indeed mediated through autophagy, we used the autophagy inhibitor 3MA or siRNA against the key autophagy regulator ATG6 (Beclin1) in PAMAM G3-treated A549 cells, and found that the viability of PAMAM G3-treated A549 cells was significantly increased by 3MA treatment (Figure 3A) or following ATG6 knockdown (Figure 3B). Thus, autophagy plays a critical role in PAMAM G3-induced cell death.

We further examined whether autophagy is a general mechanism of PAMAM-induced cell death. We analysed by western blot the lysates of A549 cells treated with other toxic PAMAM generations using the LC3 antibody (Figure 4A). Besides PAMAM G3, nanoparticle generations G4, G5, G6, G7 and G8 could all enhance the LC3-II expression level, suggesting that autophagy was induced in these cells (Figure 4A and B). Interestingly, cell death induced by toxic PAMAM generations G4, G5, G6, G7 and G8 could also be rescued by treatment with the autophagy inhibitor 3MA (Figure 4C) confirming that autophagy played a critical role in PAMAM nanoparticles-induced cell death.

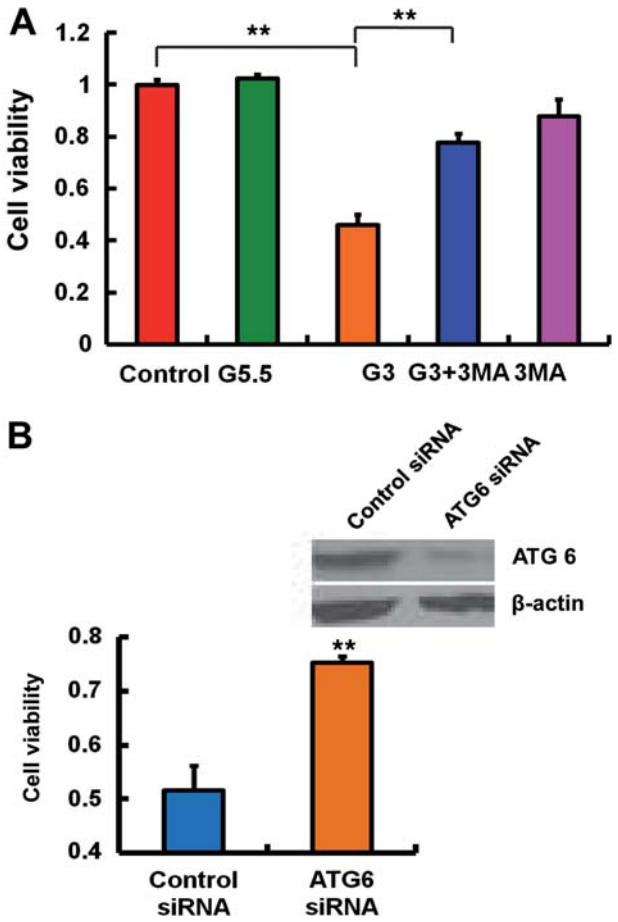

Figure 3 PAMAM G3-induced cell death is rescued by autophagy inhibitor or knockdown of ATG6. (**A**) MTT assay of A549 cells after treatment for 24 h with control, PAMAM G5.5 (100 μg/ml), PAMAM G3 (100 μg/ml), PAMAM G3 (100 μg/ml) plus 3-methyladenine (3MA, 3 mM) and 3MA (3 mM) only. $^{**}P < 0.01$. (**B**) MTT assay of A549 cells transfected with control siRNA or ATG6 siRNA after PAMAM G3 (100 μg/ml) treatment for 24 h. $^{**}P < 0.01$ compared with the control siRNA group.

Akt-TSC2-mTOR pathway is involved in the autophagic cell death induced by PAMAM

Autophagy can be triggered by inhibiting the mTOR signaling pathway (Ravikumar et al., 2004). To test whether mTOR is involved in autophagy induction by PAMAM G3, we analysed cell lysates for potential changes of proteins involved in mTOR signaling. PAMAM G3 treatment resulted in downregulation of mTOR phosphorylation, compared with control and PAMAM G5.5 treatments (Figure 5A and B), suggesting that PAMAM G3 inhibits mTOR. In addition, the phosphorylation level of S6, a substrate of mTOR, was also downregulated by PAMAM G3 (Figure 5C and D), suggesting that mTOR activity was indeed inhibited. Previous studies have shown that suppression of autophagy via mTOR can be regulated by the PI3K-Akt-TSC1/2 pathway (Meley et al., 2006; Sarbassov et al., 2005; Shinojima et al., 2007). To better understand how PAMAM G3 induces autophagy via mTOR, we performed LC3 aggregation studies in TSC2 siRNA-treated A549 cells (Figure 5E and F). The ability of PAMAM G3 to induce LC3 aggregation was significantly decreased in the TSC2 knockdown cells compared with control siRNA-treated cells (Figure 5E and F), suggesting that TSC2 is involved in PAMAM G3-induced autophagy. In addition, viability of the cells treated with TSC2 siRNA was rescued (Figure 5G). Consistent with these findings, the level of phosphorylated Akt was also markedly decreased upon PAMAM G3 treatment compared with control and PAMAM G5.5 (Figure 5H and I). Collectively, these results indicate that PAMAM G3-induced autophagy is mediated by the Akt-TSC2-mTOR pathway (Figure 5J).

Autophagy inhibitor ameliorates toxic PAMAM-induced acute lung injury in mice leading to improved survival

A549 is a human lung adenocarcinoma cell line, which is thought to originate from lung epithelial cells. We therefore speculated that PAMAM G3 treatment may also induce autophagic cell death of lung cells *in vivo*, which might in turn contribute to lung failure induced by nanoparticle exposure. To test whether PAMAM G3 could induce acute lung injury *in vivo*, we administered PAMAM G3 to mice intratracheally. PAMAM G3 instillation significantly increased lung inflammation as defined by histological pathology (Figure 6A), and elevated the wet/dry ratio of lung tissues, which was ameliorated by the autophagy inhibitor 3MA (Figure 6B). In addition, the lung elastance change caused by PAMAM G3 was partially recovered by the treatment with 3MA (Figure 6C). Importantly, mice survival rate after PAMAM G3 administration was significantly improved by 3MA treatment (Figure 6D). Taken together, our data indicate that autophagy is involved in acute lung injury induced by PAMAM nanoparticles *in vivo* and that inhibition of autophagy might have therapeutic effects on acute lung injury.

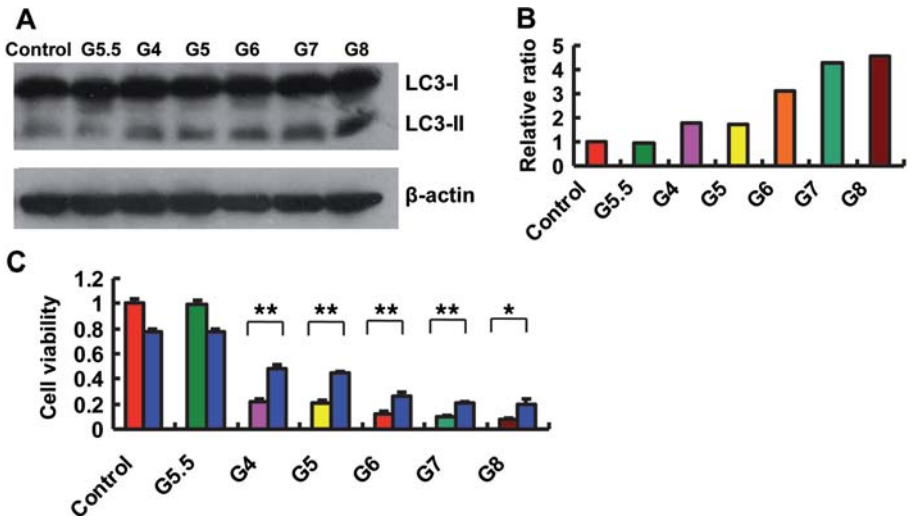

Figure 4 Autophagy is a general mechanism in toxic PAMAM nanoparticles-induced cell death. (**A**) LC3 immunoblotting of lysates of A549 cells after control, G5.5 (100 μg/ml), G4 (100 μg/ml), G5 (20 μg/ml), G6 (20 μg/ml), G7 (20 μg/ml) and G8 (20 μg/ml) treatment for 4 h. (**B**) Relative ratio of LC3-II band density to that of β-actin in control, PAMAM G5.5 (100 μg/ml), G4 (100 μg/ml), G5 (20 μg/ml), G6 (20 μg/ml), G7 (20 μg/ml) and G8 (20 μg/ml)-treated A549 cells. Band density was calculated using AlphaEaseFC software. (**C**) MTT assay of A549 cells after treatment for 24 h with control, G5.5 (100 μg/ml), G4 (100 μg/ml), G5 (20 μg/ml), G6 (20 μg/ml), G7 (20 μg/ml) and G8 (20 μg/ml) in the absence or presence of 3-methyladenine (3MA). The concentration of 3MA is 3 mM in control, G5.5, G4, G5, G6 and G7 groups, but 1 mM in G8 group. $^{**}P < 0.01$ and $^{*}P < 0.05$.

Discussion

The AKT pathway regulates many diverse biological functions. Further studies are necessary to define how PAMAM dendrimers regulate Akt-TSC2-mTOR signaling in epithelial lung tissues, which could also prove important for understanding the pathogenesis of other nanoparticle-triggered diseases. Previous reports have shown that PAMAM dendrimers enter cells through clathrin-dependent endocytosis (Kitchens et al., 2007, 2008) which also involves mTOR. How this could be linked to the effect on autophagy is unclear, although one possibility is that PAMAM dendrimers may suppress PI3K-Akt activities during endocytosis (Garcia-Regalado et al., 2008; Kitchens et al., 2007; Saeed et al., 2008; Seib et al., 2007).

Safety problems associated with nanomaterials have recently attracted great attention (Donaldson et al., 2001; Duncan and Izzo, 2005; Kagan et al., 2005; Lam et al., 2004; Nel, 2005; Nel et al., 2006; Service, 2003), highlighting the urgent need for safety protocols that protect workers and consumers as well as the environment. This study is, to our knowledge, the first report showing that autophagic cell death mediates the molecular pathogenesis of acute lung injury induced by nanoparticle PAMAM dedrimers. Our results here provide novel insight into the molecular pathogenesis of nanomaterial-induced lung injury, and contribute to a theoretical foundation for the development of safety procedures regarding nanomaterials.

Materials and methods

Animal handling

Animal experiments were conducted in the animal facility at the Institute of Basic Medical Sciences of the Peking Union Medical College in accordance with the governmental and institutional guidelines. Six- to 10-week-old male BALB/c mice were used (Vital River, Beijing). They were caged in a specific pathogen-free facility as groups of five or less and fed *ad libitum* with laboratory autoclavable rodent diet. Euthanasia was performed with pentobarbital sodium.

Cells, PAMAM dendrimer nanoparticles and antibodies

The human lung adenocarcinoma A549 cell line was purchased from ATCC, and cultured in F-12/HAM's (Hyclone) medium supplemented with 10% FBS, 100 U/ml penicillin/streptomycin at 37°C under 5% carbon dioxide. PAMAM dendrimers G1, G2, G3, G3.5, G4, G4.5, G5, G5.5, G6, G7, G7.5 and G8 were purchased from Sigma-Aldrich.

The primary antibodies used in the analysis, anti-mTOR, anti-phospho-mTOR (Ser2481), anti-AKT, anti-phospho-AKT (Ser473) and LC3B were purchased from Cell Signaling Technology. Anti-TSC2 and anti-ATG6 antibodies were purchased from Santa Cruz Biotechnology. Anti-β-actin antibody was purchased from Sigma-Aldrich. Horseradish peroxidase-conjugated secondary antibodies and western blotting luminal reagents were all from Santa Cruz Biotechnology. CellTiter 96 AQueous One Solution Cell Proliferation Assay kit was purchased from Promega Corporation. Caspase-3 fluorescence determination kit was purchased from Beijing Baosai Biotech Limited Company.

Handling of nanoparticles

PAMAM dendrimers G1, G2, G3, G3.5, G4, G4.5, G5, G5.5, G6, G7, G7.5 and G8 were bought in methanol solution. They were air

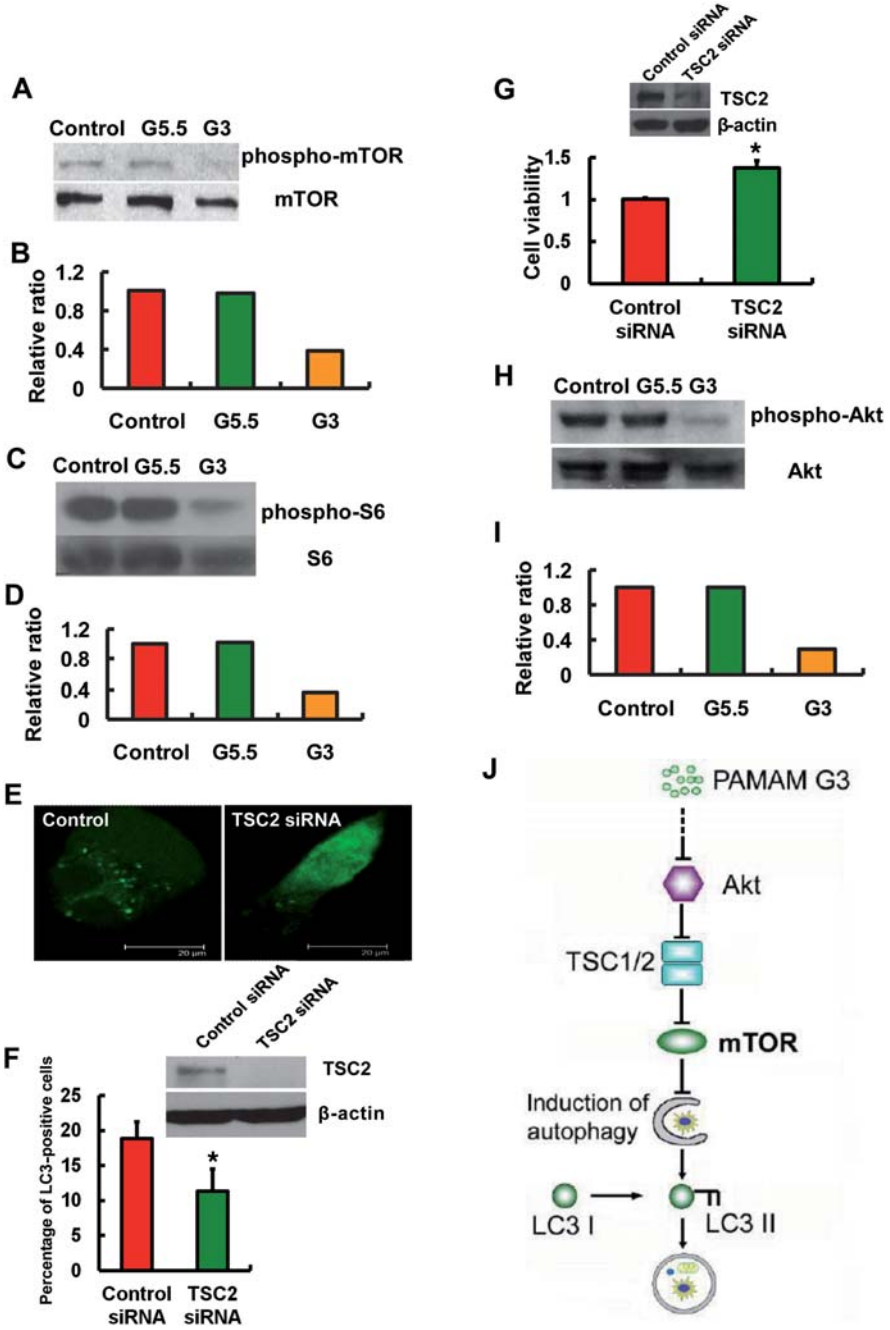

Figure 5 PAMAM G3 induces autophagy in A549 cells through the AKT-TSC-mTOR pathway. (**A**) Western blot analysis of PAMAM dendrimer (100 μg/ml)-treated and control cells probed with anti-phospho-mTOR and anti-mTOR; PAMAM dendrimer treatment was for 24 h. (**B**) Relative ratio of phospho-mTOR band density to that of mTOR in control, PAMAM G5.5 (100 μg/ml) and G3 (100 μg/ml)-treated A549 cells. Band density was calculated using AlphaEaseFC software. (**C**) Western blot analysis of PAMAM dendrimer (100 μg/ml)-treated and control cells probed with anti-phospho-S6 and anti-S6; PAMAM dendrimer treatment was for 24 h. (**D**) Relative ratio of phospho-S6 band density to that of S6 in control, PAMAM G5.5 (100 μg/ml) and G3 (100 μg/ml)-treated A549 cells. Band density was calculated using AlphaEaseFC software. (**E**) Confocal images of A549 cells, transfected with control siRNA or TSC2 siRNA, then followed by LC3-EGFP, after PAMAM G3 (30 μg/ml) treatment for 24 h. (**F**) Percentage of LC3-positive cells in control siRNA- or TSC2 siRNA-treated A549 cells after PAMAM G3 treatment for 24 h. (**G**) MTT assay of A549 cells transfected with control siRNA or TSC2 siRNA after PAMAM G3 (100 μg/ml) treatment for 24 h. *$P < 0.05$. (**H**) Western blot analysis of PAMAM G3 (100 μg/ml) treated and control cells probed with anti-phospho-Akt and anti-Akt; PAMAM dendrimer treatment was for 24 h. (**I**) Relative ratio of phospho-Akt band density to that of Akt in control, PAMAM G5.5 (100 μg/ml) and G3 (100 μg/ml)-treated A549 cells. Band density was calculated using AlphaEaseFC software. (**J**) Schematic representation of the signaling pathway involved in PAMAM G3-induced autophagy.

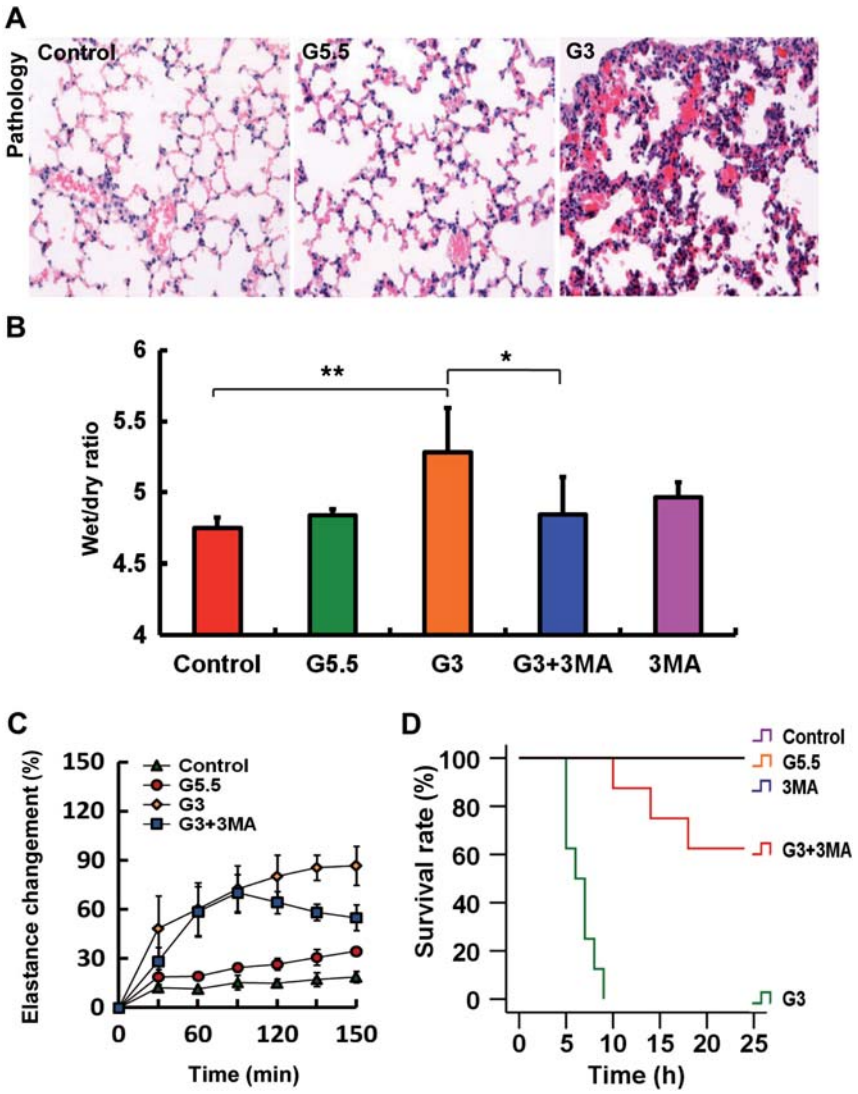

Figure 6 Autophagy plays a critical role in PAMAM G3-induced acute lung injury in mice. (**A**) HE staining of Balb/c mice lung tissues after intratracheal administration of control vehicle, PAMAM G5.5 (50 mg/kg) and PAMAM G3 (50 mg/kg); PAMAM dendrimer treatment was for 4 h. Original magnifications are 200X. (**B**) Wet/dry ratios of lung tissues of Balb/c mice after intratracheal administration of control vehicle, PAMAM G5.5 (50 mg/kg), PAMAM G3 (50 mg/kg) and PAMAM G3 (50 mg/kg) plus intraperitoneal injection of 3-methyladenine (3MA, 15 mg/kg), as well as 3MA (15 mg/kg) injection only; PAMAM dendrimer treatment was for 16 h. $^{**}P < 0.01$ and $^{*}P < 0.05$. (**C**) Changes of lung elastance in Balb/c mice after intratracheal administration of control vehicle, PAMAM G5.5 (50 mg/kg), PAMAM G3 (50 mg/kg) and PAMAM G3 (50 mg/kg) plus intraperitoneal injection of 3MA (15 mg/kg). (**D**) Survival rate of Balb/c mice after intratracheal administration of control vehicle, PAMAM G5.5 (50 mg/kg), PAMAM G3 (50 mg/kg) and PAMAM G3 (50 mg/kg) plus intraperitoneal injection of 3MA (15 mg/kg) as well as 3MA (15 mg/kg) injection only.

dried on a clean bench for 24 h to remove methanol. As vehicle, PBS was then added to dissolve the nanoparticles.

MTT assay

A549 cells were seeded in 96-well plate at 1×10^5/ml. PAMAM G1, G2, G3, G3.5, G4, G4.5, G5, G5.5, G6, G7, G7.5 and G8, or an equal volume of control (PBS) was added to the wells in the next day. In the PAMAMs plus 3-MA group, 3-MA was added 1 h before PAMAMs. Each group had triplicate wells. After 24 h, 20 μl of CellTiter 96 AQueous One Solution Cell Proliferation Assay solution was added to each well, and incubated for another 2 h. Absorbance was then recorded at 490 nm.

DNA extraction

A549 cells were seeded in 6-cm plate at 1×10^6/ml. DMSO 6%, PAMAM G3 (100 μg/ml) or an equal volume of control was added to the plate on the next day. Cells were harvested and DNA was extracted as previously described.

Caspase-3 activity determination

A549 cells were seeded in 6-cm plate at 1×10^6/ml. DMSO 6%, PAMAM G3 (100 μg/ml), PAMAM G5.5 (100 μg/ml) or an equal volume of control was added to the plate on the next day. After 24 h, cells were lysed and caspase-3 activity was determined

using caspase-3 fluorescence kit following manufacturer's protocol.

Western blotting

A549 cells were seeded at 1×10^5/ml in 12-well plate. PAMAM G3 (100 μg/ml), PAMAM G5.5 (100 μg/ml) or an equal volume of control was added to the wells on the next day. After 24 h, cells were lysed in lysis buffer, denatured at 97°C for 10 min and subjected to western blot analysis. Band density was calculated using AlphaEaseFC software.

Transmission electron microscopy

A549 cells were seeded in 6-well plate at 2×10^5/ml. PAMAM G3 (100 μg/ml), PAMAM G5.5 (100 μg/ml) or an equal volume of control was added to the wells in the next day. In the PAMAM G3 plus 3-MA group, 3-MA (10 mM) was added 1 h before PAMAM G3. After 24 h, cells were trypsin-digested and centrifuged at 800 *g* for 5 min. The supernatant was discarded and the cells were fixed with 2.5% glutaraldehyde in 0.1 M sodium dihydrogen phosphate (pH 7.4). The samples were then fixed in 1% OsO_4 for 1 h and dehydrated by increasing concentrations of acetone, and gradually infiltrated with epoxy resin. Ultra-thin sections were obtained and stained with uranyl acetate and lead citrate. A cell showing two or more autophagosomes was defined to be an autophagy-positive cell.

LC3-EGFP counting

A549 cells were seeded on coverslips in 24-well plate. One day later, LC3-EGFP plasmid was transfected. Forty-eight hours after transfection, PAMAM G3 (30 μg/ml), PAMAM G5.5 (30 μg/ml) or an equal volume of control was added to the wells. In the PAMAM G3 plus 3MA group, 3MA (10 mM) was added 1 h before PAMAM G3. After 24 h, EGFP dots in the cell were counted using a Leica laser-scanning spectrum confocal system linked to a microscope (Leica TCS PS2). Images were captured under the 100X oil objective (Plan-Apo 1.4) with the confocal acquisition software LCS (Leica). A cell containing 10 or more EGFP dots was defined to be an LC3-positive cell.

LC3-EGFP counting in TSC2 siRNA-treated A549 cells

A549 cells were seeded in 24-well plate the day before being transfected with siRNA against TSC2 (50 nM, Santa Cruz Biotechnology) or control siRNA using lipofectamin 2000 (Invitrogen). Twenty-four hours after TSC2 transfection, cells were transfected with LC3-EGFP plasmid. Another 36 h later, the effect of the siRNA was determined by western blot with anti-TSC2 antibody. In parallel, cells were treated with PAMAM G3 (30 μg/ml). The accumulation of EGFP-LC3 was determined by Leica Confocal Microscope as described above.

MTT assay in TSC2 siRNA-treated cells

A549 cells were seeded in 24-well plate the day before being transfected with siRNA against TSC2 (50 nM, Santa Cruz Biotechnology) or control siRNA using lipofectamine 2000 (Invitrogen). Another 48 h later, the effect of the siRNA was determined by western blot with anti-TSC2 antibody. In parallel, 24 h after transfection, cells were trypsin-digested and seeded on 96-well plate. PAMAM G3 (100 μg/ml) was added to the TSC2 siRNA and control siRNA group in the next day, and the MTT assay was conducted in the following day.

MTT assay in ATG6 siRNA-treated cells

A549 cells were seeded in 24-well plate. Twenty-four hours later, cells were transfected with siRNA against ATG6 (100 μM, Santa Cruz Biotechnology) or control siRNA. Another 48 h later, the effect of the siRNA was determined by western blot with anti-ATG6 antibody. In parallel, 24 h after transfection, cells were trypsin-digested and seeded on 96-well plates. PAMAM G3 (100 μg/ml) was added to the ATG6 siRNA and control siRNA group in the next day, and the MTT assay was conducted in the following day.

Mice lung tissue histopathological examination

Four hours after intratracheal administration of control, PAMAM G5.5 (50 mg/kg) or PAMAM G3 (50 mg/kg), the Balb/c mice were sacrificed. Lungs were fixed in formalin for 48 h and then embedded in paraffin. Ultra-thin sections were obtained and stained with hematoxylin–eosin. Each slide was independently examined by three different pathologists.

Mice lung wet/dry ratio assay

The Balb/c mice were randomly grouped. After anesthesia by intraperitoneal injection with 1% pentobarbital sodium solution, they were intratracheally administered with 10 μl of control, PAMAM G5.5 (50 mg/kg) or PAMAM G3 (50 mg/kg). In the 3MA-only group, 3MA (15 mg/kg) was injected intraperitoneally. In the rescue group, 1 h after intraperitoneal injection with 3MA (15 mg/kg), PAMAM G3 (50 mg/kg) was administered intratracheally. After spontaneous breathing for 16 h, mice were sacrificed and the lungs were assessed for the wet weight. To obtain the dry weight, the lungs of mice were dried in an oven at 55°C for 24 h.

Assay for mice lung elastance changes

The Balb/c mice were randomly grouped. After anesthesia by intraperitoneal injection with 1% pentobarbital sodium solution, they were intratracheally administered with 10 μl of control, PAMAM G5.5 (50 mg/kg) and PAMAM G3 (50 mg/kg), respectively, with 3 s 30 cm H_2O pressure followed by 2 min 25 cm H_2O pressure ventilation. In the 3-methyladenine (3MA) rescue group, 3MA (15 mg/kg) was injected intraperitoneally before PAMAM G3 (50 mg/kg) was administered intratracheally. Then elastance was tested by BUXCO pulmonary function testing (PFT) every 30 min during the spontaneous breathing period for 3 h.

Mice survival rate assay

The Balb/c mice were randomly grouped. After anesthesia by intraperitoneal injection with 1% pentobarbital sodium solution they were intratracheally administered with 20 μl of control, PAMAM G5.5 (50 mg/kg) or PAMAM G3 (50 mg/kg). 3MA (15 mg/kg) was injected twice intraperitoneally, 12 h and 1 h, respectively, before intratracheal administration of PAMAM G3 (50 mg/kg). The survival/death status of mice was recorded every 1 h for a total of 24 h. The data were analysed by SPSS software.

Statistical analyses

All data were shown as mean ± S.E.M. and statistical analyses were conducted using the student *t*-test.

Acknowledgements

We thank Peng Yang, Zongsheng Han, Kangtai Liu, Wen Xi, Xiangwu Ju, Huan Wang, Rui Lu, Ziang Pan, Ruihong Sheng and Xu Liu for technical support. We thank Josef Penninger and Helen Pickersgill for helpful discussions and editing the manuscript.

Conflict of interest: none declared.

Funding

This work is supported by National Natural Science Foundation of China (30625013 and 30721063) and Ministry of Science and Technology of China (2009CB522105 and 2006CB933203). D.L. acknowledges the support from Science and Technology Commission of Shanghai Municipality (07pj14096).

References

Aita, K., Irie, H., Tanuma, Y., Toida, S., Okuma, Y., Mori, S., and Shiga, J. (2005). Apoptosis in murine lymphoid organs following intraperitoneal administration of dimethyl sulfoxide (DMSO). Exp. Mol. Pathol. *79*, 265–271.

Asanuma, K., Tanida, I., Shirato, I., Ueno, T., Takahara, H., Nishitani, T., Kominami, E., and Tomino, Y. (2003). MAP-LC3, a promising autophagosomal marker, is processed during the differentiation and recovery of podocytes from PAN nephrosis. FASEB J. *17*, 1165–1167.

Baehrecke, E.H. (2005). Autophagy: dual roles in life and death? Nat. Rev. *6*, 505–510.

Bergmann, A. (2007). Autophagy and cell death: no longer at odds. Cell *131*, 1032–1034.

Chen, Y., Yang, L., Feng, C., and Wen, L.P. (2005). Nano neodymium oxide induces massive vacuolization and autophagic cell death in non-small cell lung cancer NCI-H460 cells. Biochem. Biophys. Res. Commun. *337*, 52–60.

Cheng, Y., Li, M., and Xu, T. (2008). Potential of poly(amidoamine) dendrimers as drug carriers of camptothecin based on encapsulation studies. Eur. J. Med. Chem. *43*, 1791–1795.

Cheng, Y., Man, N., Xu, T., Fu, R., Wang, X., Wang, X., and Wen, L. (2007). Transdermal delivery of nonsteroidal anti-inflammatory drugs mediated by polyamidoamine (PAMAM) dendrimers. J. Pharm. Sci. *96*, 595–602.

Donaldson, K., Stone, V., Clouter, A., Renwick, L., and MacNee, W. (2001). Ultrafine particles. Occup. Environ. Med. *58*, 211–216, 199.

Duncan, R., and Izzo, L. (2005). Dendrimer biocompatibility and toxicity. Adv. Drug. Deliv. Rev. *57*, 2215–2237.

Freitas, R.A., Jr. (2005). What is nanomedicine? Nanomedicine *1*, 2–9.

Gao, Y., Gao, G., He, Y., Liu, T., and Qi, R. (2008). Recent advances of dendrimers in delivery of genes and drugs. Mini. Rev. Med. Chem. *8*, 889–900.

Garcia-Regalado, A., Guzman-Hernandez, M.L., Ramirez-Rangel, I., Robles-Molina, E., Balla, T., Vazquez-Prado, J., and Reyes-Cruz, G. (2008). G protein-coupled receptor-promoted trafficking of Gβ1γ2 leads to AKT activation at endosomes via a mechanism mediated by Gβ1γ2-Rab11a interaction. Mol. Biol. Cell *19*, 4188–4200.

Gelperina, S., Kisich, K., Iseman, M.D., and Heifets, L. (2005). The potential advantages of nanoparticle drug delivery systems in chemotherapy of tuberculosis. Am. J. Resp. Crit. Care Med. *172*, 1487–1490.

Hecht, S., and Frechet, J.M. (2001). Dendritic encapsulation of function: applying nature's site isolation principle from biomimetics to materials science. Angewandte. Chemie. (International ed.) *40*, 74–91.

Kagan, V.E., Bayir, H., and Shvedova, A.A. (2005). Nanomedicine and nanotoxicology: two sides of the same coin. Nanomedicine *1*, 313–316.

Kitchens, K.M., Foraker, A.B., Kolhatkar, R.B., Swaan, P.W., and Ghandehari, H. (2007). Endocytosis and interaction of poly (amidoamine) dendrimers with Caco-2 cells. Pharm. Res. *24*, 2138–2145.

Kitchens, K.M., Kolhatkar, R.B., Swaan, P.W., and Ghandehari, H. (2008). Endocytosis inhibitors prevent poly(amidoamine) dendrimer internalization and permeability across Caco-2 cells. Mol. Pharm. *5*, 364–369.

Lam, C.W., James, J.T., McCluskey, R., and Hunter, R.L. (2004). Pulmonary toxicity of single-wall carbon nanotubes in mice 7 and 90 days after intratracheal instillation. Toxicol. Sci. *77*, 126–134.

Malik, N., Wiwattanapatapee, R., Klopsch, R., Lorenz, K., Frey, H., Weener, J.W., Meijer, E.W., Paulus, W., and Duncan, R. (2000). Dendrimers: relationship between structure and biocompatibility *in vitro* and preliminary studies on the biodistribution of 125I-labelled polyamidoamine dendrimers *in vivo*. J. Contr. Release *65*, 133–148.

Meley, D., Pattingre, S., and Codogno, P. (2006). [PI3 kinases and the control of autophagia]. Bull. du. Cancer *93*, 439–444.

Nel, A. (2005). Atmosphere. Air pollution-related illness: effects of particles. Science *308*, 804–806.

Nel, A., Xia, T., Madler, L., and Li, N. (2006). Toxic potential of materials at the nanolevel. Science *311*, 622–627.

Nigavekar, S.S., Sung, L.Y., Llanes, M., El-Jawahri, A., Lawrence, T.S., Becker, C.W., Balogh, L., and Khan, M.K. (2004). 3H dendrimer nanoparticle organ/tumor distribution. Pharm. Res. *21*, 476–483.

Ravikumar, B., Vacher, C., Berger, Z., Davies, J.E., Luo, S., Oroz, L.G., Scaravilli, F., Easton, D.F., Duden, R., O'Kane, C.J., et al. (2004). Inhibition of mTOR induces autophagy and reduces toxicity of polyglutamine expansions in fly and mouse models of Huntington disease. Nat. Genet. *36*, 585–595.

Saeed, M.F., Kolokoltsov, A.A., Freiberg, A.N., Holbrook, M.R., and Davey, R.A. (2008). Phosphoinositide-3 kinase-Akt pathway controls cellular entry of Ebola virus. PLoS Pathogens *4*, e1000141.

Sarbassov, D.D., Ali, S.M., and Sabatini, D.M. (2005). Growing roles for the mTOR pathway. Curr. Opin. Cell Biol. *17*, 596–603.

Seib, F.P., Jones, A.T., and Duncan, R. (2007). Comparison of the endocytic properties of linear and branched PEIs, and cationic PAMAM dendrimers in B16f10 melanoma cells. J. Contr. Release *117*, 291–300.

Seleverstov, O., Zabirnyk, O., Zscharnack, M., Bulavina, L., Nowicki, M., Heinrich, J.M., Yezhelyev, M., Emmrich, F., O'Regan, R., and Bader, A. (2006). Quantum dots for human mesenchymal stem cells labeling. A size-dependent autophagy activation. Nano Lett. *6*, 2826–2832.

Service, R.F. (2003). American Chemical Society Meeting. Nanomaterials show signs of toxicity. Science *300*, 243.

Shinojima, N., Yokoyama, T., Kondo, Y., and Kondo, S. (2007). Roles of the Akt/mTOR/p70S6K and ERK1/2 signaling pathways in curcumin-induced autophagy. Autophagy. *3*, 635–637.

Svenson, S., and Tomalia, D.A. (2005). Dendrimers in biomedical applications: reflections on the field. Adv. Drug. Delivery Rev. *57*, 2106–2129.

Trubiani, O., Pieri, C., Rapino, M., and Di Primio, R. (1999). The *c-myc* gene regulates the polyamine pathway in DMSO-induced apoptosis. Cell Proliferation *32*, 119–129.

Xu, R., Wang, Y., Wang, X., Jeong, E.K., Parker, D.L., and Lu, Z.R. (2007). In vivo evaluation of a PAMAM-cystamine-(Gd-DO3A) conjugate as a biodegradable macromolecular MRI contrast agent. Exp. Biol. Med. *232*, 1081–1089.

Zabirnyk, O., Yezhelyev, M., and Seleverstov, O. (2007). Nanoparticles as a novel class of autophagy activators. Autophagy. *3*, 278–281.